Nikolaj Višniakov[a], Gediminas Mikalauskas[a], Jelena Škamat[b], Raimonda Lukauskaitė[a], Olegas Černašėjus[a], Vitalijus Rudzinskas[a], Renata Boris[b]
[a]Faculty of Mechanics, Vilnius Gediminas Technical University, Vilnius, Lithuania
[b]Institute of Thermal Insulation, Vilnius Gediminas Technical University, Vilnius, Lithuania

Thermite welding of Cu–Nb microcomposite wires

Thermite welding of Cu–Nb microcomposite wires was investigated. Suitable compositions of thermite material and slag were determined from the equation of the exothermic combustion synthesis reaction. The phase compositions of the thermite mixture and slag determined by X-ray diffraction analysis correspond to those assessed from the equation. According to non-destructive radiographic testing, the joint structure does not have welding defects. Microstructural examination of the joint cross-section with scanning electron microscopy showed that the Cu–Nb wire retained its shape and microstructure and only a thin surface layer of wire was melted during welding. The difference in electrical resistances of the conductor and welded joint was below 20 %. The thermite joint can withstand a maximum load equal to 62.5 % of the load-bearing capacity of microcomposite conductor.

Keywords: Cu–Nb microcomposite wire; Welded joint; Thermite welding; Pulsed magnet

1. Introduction

Magnetic field is a basic tool for fundamental research in physics, biology, bioengineering, chemistry, biochemistry, geochemistry, etc. Huge magnet systems are used in such grand projects as CERN, ITER, and ARC. Electromagnetic fields are also widely used in industry for such processes as induction welding, sealing, heat treatment, magnetic levitation, electromagnetic forming, etc. Generating a high magnetic field is a complicated task due to the high requirements of equipment, materials, energy and other resources. Nowadays, compact and low-cost pulsed magnets find broad applications both in science and in industry [1, 2]. This energy-efficient equipment can generate record magnetic fields and require a minimal amount of infrastructure. Among the most important parts of pulsed and static magnetic field generators are their inductors, frequently solenoids. Experiments, research, and design improvement in this area are being carried out very intensively, but the problem remains relevant [3]. Cylindrical multilayer solenoids are the most popular in impulse magnet design. Currently, investigations in this field are focussed on the development of pulsed magnets that are able to generate a magnetic flux of $B = 100$ T for 10 ms [4]. For this task, four types of composite conductors are being used: Cu–Nb and Cu–Ag microcomposites and GlidCop and CuSS macrocomposites due to their extremely high strength and good conductivity [2, 5–7]. The ultimate tensile strength (R_m) of Cu–Nb conductors reaches 1100 MPa, with yield strength (R_p) of 850 MPa, percentage elongation after fracture (A) of 2.5–10 %, and electrical conductivity of 67–70 % IACS (International Annealed Copper Standard). The structure of Cu–Nb microcomposite conductors comprises a Cu matrix with very thin Nb fibres placed within them. The Nb fibres strengthen the copper matrix, ensure a higher strength of conductor, and do not hinder the movement of electrons, i. e. the flow of electric current [8]. At present, essentially two technologies are used to produce Cu–Nb composite conductors: "fusion-deformation" (in situ) [9, 10] and "assembly-deformation" [8].

The solenoids of various high magnetic field systems consist of separate magnet sections, which have to be connected [11–13]. High technical requirements are applied to the joints, among which the complexity of electrical parameters, mechanical properties, and reliability are the most important. As a result, the development of reliable non-destructive joints is focussed on. Typically, conductors in pulsed power systems are joined with screws or soldered joints, which have limited reliability [14, 15]. As alternatives, welding and pressing are the most progressive technologies for joining conductors. Material connection at the atomic level occurs either by melting and subsequent cooling of the metal (fusion welding) or by pressing the elements (pressure welding) [16]. An intermediate position between these welding methods is thermite welding where a self-propagating solid-state reaction is used to form the joint. Thermite welding seems to be the most practical solution among the special welding methods. Thermite reactions are also used in the production of Cu–Nb alloys. Thermite smelting (via the aluminothermic reduction of mixed CuO, Nb_2O_5 oxides, Al powder, and CaO flux) has been described earlier [17]. Exothermic reactions of nanothermites based on Al–CuO are relevant in the area of self-propagating high-temperature synthesis (SHS), combustion synthesis (CS), and mechanically induced self-propagating reactions (MSR) [18–21]. Therefore, an analogous technology could hypothetically be used to join Cu–Nb microcomposite conductors. However, the basis for thermite welding is the "Goldschmidt" reaction [16], while Al is the most popular and least expensive of metals used in thermal reactions. Various additives (ferroalloys Fe–Mn or Fe–Si, silicide $CaSi_2$, etc.) are added into the thermite mixture. As a result, such compounds improve the characteristics of welded

joints, reduce metal consumption, reduce the temperature of exothermal reactions, and improve slag properties. The thermite mixture with up to 90 wt.% Cu oxide and Cu powder, 11 wt.% Al or its alloy, and 18 wt.% other additives for multi-thread and solid profile Cu conductors welding is useful in practice [22–30].

The effect of oxide film on the surface of welded metal can be reduced by using special fluxes. Neutral fluxes containing reactive fluoride salts (CaF_2) can strip oxide films from copper-based alloys, thus permitting entrained metallic droplets to return to the melt phase. CaF_2 can be used to lower the fusion point and increase the fluidity of the reaction products (slag). However, in practice, thermite welding of copper conductors is performed without additional fluxes since it has been determined that the quality of thermite joint does not depend on the use of flux [31]. Nevertheless, CaF_2 can be used in the thermite mixture for the same reason. Moreover, many reactive metals can be used instead of Al as it is possible to create complex thermite systems with two chemically independent reactions [21]. For example, the mixture of Sn and CuO is also classified as a thermite that can revivify Cu according to the Ellingham diagram [31]. However, the heat emitted by this exothermal reaction is low. Sn reduces the melting point of Cu–Sn alloys, and increases the elasticity and strength of the metal relative to pure Cu. Alloys of Cu or Fe with Sn are used for metal disc inserts. For example, the Cu alloy with Sn and P (phosphoric-oxidised copper) was popular earlier [32]. The mould is additionally deoxidised since the acquired alloy includes phosphorus. P improves the viscosity of the liquid metal, its weldability, and the mechanical characteristics and quality of the welded joint. However, a P concentration of only 0.05 wt.% decreases the electrical and thermal conductivity by 20–30 % [33]. Therefore, the P concentration in Cu and its alloys for electrical engineering must be limited to 0.001 wt.%. Cu–Sn alloys (phonoelectric bronze) are used for trolleybus electrical lines [34]. Therefore, Fe and Sn alloy disc inserts may be used for thermite welding. A small amount of Fe impurity does not reduce the quality of a thermite joint. Another often-used strategy to lower the temperature of the thermite reaction and its speed is the introduction of inert compounds into the thermite mixture. Al_2O_3, CaO, and SiO_2 impurities (slag compounds) – which can usually be found in various thermite mixtures – reduce the reaction speed and combustion temperature. Inert additives located between reactant particles decrease the contact surface and consequently the overall reaction rate [21]. The thermite mixture with analogous compounds could also be applied for joining Cu–Nb conductors because the base of Cu–Nb microcomposite conductors is Cu. Our review of theory, technical literature, and articles with experimental research results shows that data regarding Cu–Nb microcomposite welding possibilities are not sufficient. Therefore, the purpose of the research carried out in this work was to estimate the quality and properties of Cu–Nb microcomposite conductor thermite joints.

2. Materials and methods

Commercially available Cu-18Nb (wt.%) wire with 2.4 mm × 4.2 mm cross-section was used for this research. The wire was manufactured using the "assembly-deformation" method. The mechanical properties of this wire are: yield strength (R_p) 830–850 MPa, ultimate tensile strength (R_m) 1 120 MPa and percentage elongation after fracture (A) 4.2 % [35]. The structure of the microcomposite consisted of Nb fibres <15 nm and a copper matrix covered with a thin Cu cladding [8]. The composition of the thermite mixture was selected in accordance with known thermite mixtures for copper alloys and the particularity of the Cu–Nb microcomposite structure. Along with the oxidiser (CuO and/or Cu_2O) and fuel (Al), the thermite mixture for copper alloys often contains $CaSi_2$ (normally, more than 5 % of the total mass). The combination of $CaSi_2$ and Al (as fuel) at molar ratios from 0.25 : 1 to 16 : 1 ensures that during the exothermal reaction of the mixture a high temperature will be reached and the Al_2O_3–CaO–SiO_2 slag system will form.

The Al_2O_3–CaO–SiO_2 slag system has a lower melting point, lower density, better separation and improved fluidity, than the crystalline Al_2O_3 slag. Al_2O_3 has a density of 3 960 kg · m^{-3} and melting point 2 054 °C. $CaSi_2$ also has a positive effect on the ignition and combustion temperatures. In practice, an Al and $CaSi_2$ combination with a molar ratio of 2 : 1 is used. In such a case, a glassy amorphous slag is formed during the thermite reaction, which has the formula of the mineral anorthite ($CaAl_2Si_2O_8$). An anorthite slag has a composition of CaO 20.14 wt.%, SiO_2 43.17 wt.%, Al_2O_3 36.69 wt.%. Anorthite has a density of 2 700 kg · m^{-3} and melting point of 1 550 °C. According to the CaO–Al_2O_3–SiO_2 phase diagram [36], anorthite crystallisation is obtainable in a quite narrow range of composition. Therefore, accurate selection of the mixture composition is required. Anorthite slag formation is more advantageous than ceramic Al_2O_3 slag because the anorthite formation reaction itself is an exothermic process, which increases the temperature of the overall reaction and assists with the fusing of liquid metal during the exothermic reaction [22, 23]. Previous studies [22–34] have demonstrated that the adiabatic reaction temperature of the thermite mixture (maximum temperature that can be reached in a composition of the invention during reaction) has to be higher than 2 083 °C for complete slag separation. This temperature also must not exceed 2 573 °C because in such a case too much copper vapour will be generated if the reaction is performed open to the atmosphere. The temperature of this reaction must also exceed the melting points of all metals in the mixture without exceeding their boiling points. As is known, the melting point of Cu is 1 085 °C and its boiling point 2 567 °C. The exothermic combustion synthesis reactions can be expressed by Eq. (1) [22, 23].

$$\alpha M_xO_y + 2\mathrm{Al} + \beta\mathrm{CaSi_2} + \sum_i x_iM_i \xrightarrow{T_{ig}} \mathrm{Al_2O_3} + \beta\mathrm{CaO} + 2\beta\mathrm{SiO_2} + \alpha xM + \sum_i x_iM_i \xrightarrow{T_c} \mathrm{Ca}_\beta\mathrm{Al_2Si}_{2\beta}\mathrm{O}_{3+5\beta} + axM + \sum_i x_iM_i \quad (1)$$

where M – elemental or alloyed metals; α, β, and x_1 – numbers related by $\alpha y = 3 + 5\beta$ to correspond to mass conservation; T_{ig} – ignition temperature of the reactant mixture of M_xO_y, Al, $CaSi_2$, and M; and T_c – combustion temperature

reached in the process, where reactions between the slag phases continue forming ternary compounds with an overall composition of $Ca_{\beta}Si_2Si_{2\beta}O_{3+5\beta}$.

The ratio of thermite reaction products (metal and slag) must be within a particular range according to the research results published in Refs. [22–30]. The thermite mixture will have a high adiabatic reaction temperature (2449 °C), good ignition, and perfect slag separation if the metal and slag ratio is in the range (Cu up to 85 wt.%, slag no less than 15 wt.%). Suitable compositions having suitable combustion temperatures can be determined from Eq. (1), the calculation of adiabatic reaction temperature, and experiments. A thermite mixture should have a high reaction temperature (2449 °C – 2567 °C), Cu output up to 85 wt.%, slag no less than 15 wt.%, and Al to $CaSi_2$ molar ratio of 2 : 1. For the present experiments, a thermite mixture was prepared according to the exothermic combustion synthesis reaction equation and conditions listed above. The composition of the prepared thermite mixture is listed in Table 1.

The phase composition of the thermite was determined by X-ray diffraction (XRD) analysis using an X-ray diffractometer (SmartLab (Rigaku)) with a 9 kW rotating Cu anode X-ray tube. For the analysis, the PDF-4+ (2016) crystalline compound database was used. The XRD pattern of the created mixture is presented in Fig. 1.

A special flame-resistant graphite mould was used for the thermite welding (with intermediate moulding) of Cu–Nb wire butt connections. A portion of thermite, appropriate for the volume of the joint, was poured into a crucible mould and ignited. The Erico Cadweld (the Netherlands) electric ignition system was used to ignite the thermite mixture. A thin Fe-50Sn (wt.%) disc was inserted at the bottom of the crucible before the thermite mixture was poured into a mould.

Non-destructive testing was performed to ensure that the welded joints were of good quality. A GE ERESCO 42MF4 (US) radiographic device was used.

Table 1. The phase composition of the thermite mixture.

Compounds	$CuAl_2$	$CaSi_2$	Cu_2O	Sn	CaF_2
wt.%	8.65	6.90	82.00	2.20	0.25

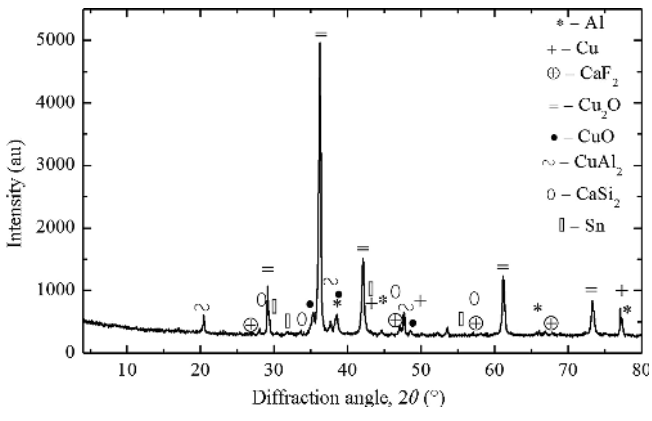

Fig. 1. X-ray diffraction pattern of thermite mixture.

The metal to slag mass ratio after the thermite reaction was determined using analytic balances (KERN EW620-3NM (Germany)).

XRD analysis of the slag was performed with a diffractometer (DRON-7 (Russia)) using Cu-K_{α} radiation (λ = 0.1541837 nm) with anode voltage of 30 kV, anode current of 12 mA, and goniometer slits of 0.5, 1.0, and 1.5 mm. The ICDD database was used to analyse the XRD data.

The microstructure of the joint and fracture surface was analysed by means of scanning electron microscopy (SEM). A scanning electron microscope (JEOL JSM-7600 (Japan)) equipped with an energy dispersive X-ray spectrometer (EDS) for chemical microanalysis (Oxford INCA Energy X-Max20 (UK)) was used.

To measure electrical resistance, three fragments of Cu–Nb wire were taken and three welded butt joints were prepared for each joining (resistance welding, thermite welding, soldering) method. Each sample was of length 30 cm. The electrical resistance was measured by the four-probe method using a U2810D Digital LCR Meter Tester (China). The measurement technique and scheme are presented in Ref. [32].

To estimate resistive heating of the thermite welded, resistance welded and soldered Cu-Nb conductors, the method applicable for electrical connections [37, 38] was used. Joule heating of the three samples was experimentally established using a welding rectifier VDU-305 (USSR) and thermal imaging infrared camera (model Flir-E49001). The samples were heated with a 200 A electrical current. The temperature distribution at the beginning of the experiment and after every 30 s was registered.

The mechanical properties of the thermite welding joints were determined via tensile testing. Three welded butt joints, each 30 cm in length, were tested. A universal tensile press TIRAtest 2300 (Germany) with a computerised measuring system, an analogue–digital converter (Spider-8) with data registration, operating software (Katman–Express) and dynamometer up to 20 kN (precision 0.5 %) was used.

The hardness of the weld metal was measured on the polished surface of the joint cross-section via Vickers hardness testing. A universal hardness tester Zwick/Roell ZHU (Germany) was used. The 98.07 N nominal value of test force and 30 s duration time of test were used.

3. Results and discussion

The general view of a welded joint is shown in Fig. 2. The joint displays the Cu-rich metal ingot (weld) with the included ends of Cu–Nb wire from two opposite sides (Fig. 2a). The shape of the weld repeats the form of the graphite mould; the size of the weld is about $10 \times 12 \times 18$ mm (after the slag has been removed). The cross-section of the weld was ~ 100 mm^2. No visible macro-defects (pores, inclusions, other discontinuities) were observed from the cross-section of the joint (Fig. 2b). It is also clear from this view that the conductor retained its initial shape. The quality of the welded joints was evaluated through radiographic non-destructive control. Welding imperfections were not detected in the welded joints, indicating that the thermite composition selected is suitable for good quality joining. The Cu metal weight was ~ 76 wt.% and slag ~ 24 wt.% of the obtained reaction products. The slag composition ac-

cording to XRD analysis (see Fig. 3) corresponds to products of the $CaO–Al_2O_3–SiO_2$ system, defined in Eq. (1). In the diffraction curve, the easily identifiable peaks correspond to CaO, SiO_2, Al_2O_3 and $CaAl_2Si_2O_8$.

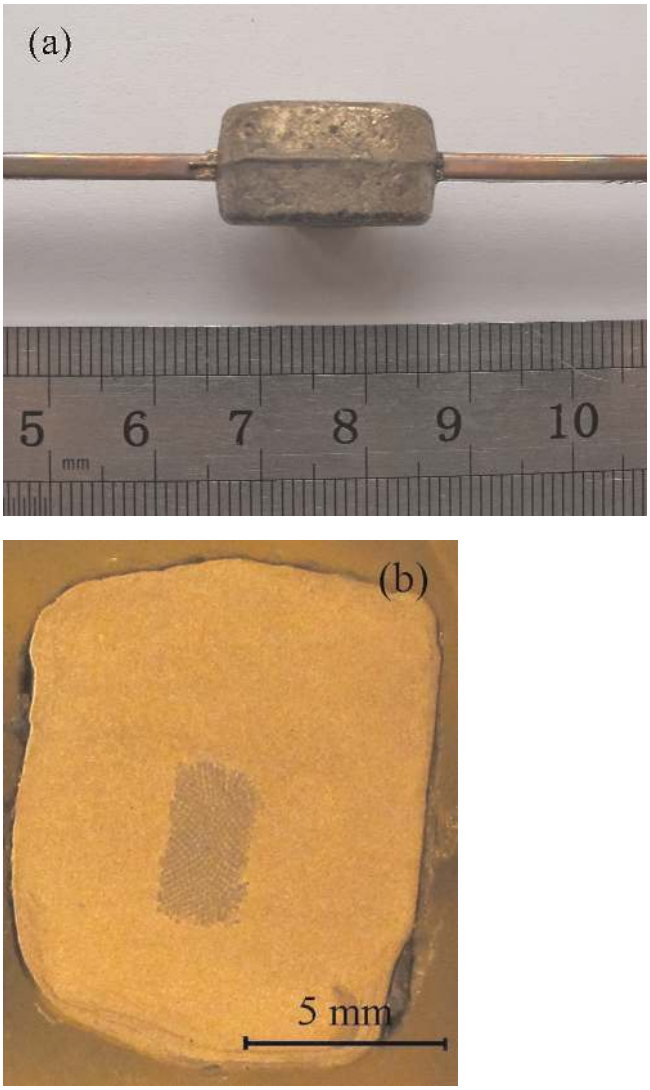

Fig. 2. Thermite welded joint of Cu–Nb microcomposite wire: (a) front view; (b) cross- section of joint.

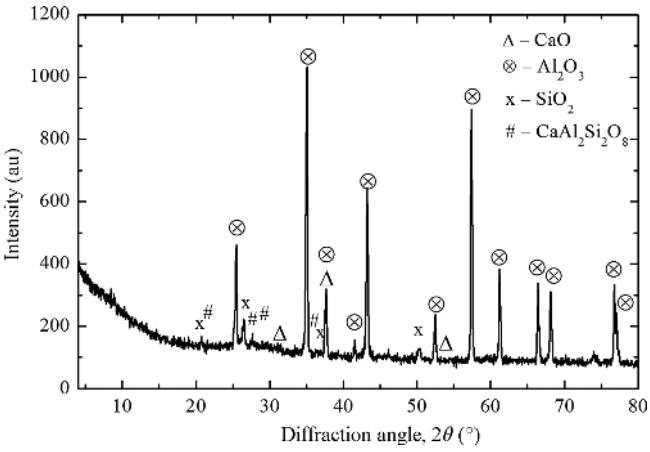

Fig. 3. X-ray diffraction pattern of slag.

The microstructure of a thermite joint is shown in Fig. 4. It can be seen from Fig. 4a that a solid joint with no discontinuity at the interface was formed by thermite welding. The conductor is surrounded by a Cu-rich metal ingot (denoted "thermite weld" in Fig. 4a and b), which crystallised from the liquid state during the exothermic combustion synthesis reaction. According to the EDS spectrum analysis (see Table 2), the thermite weld contained ~98 % Cu and an insignificant amount (~2 %) of other elements. The amount of Sn in the weld composition was about 0.21 wt.% (Table 2). This element is very soluble in liquid Cu. According to the Cu–Sn phase transition diagram [39], Cu–Sn alloys with

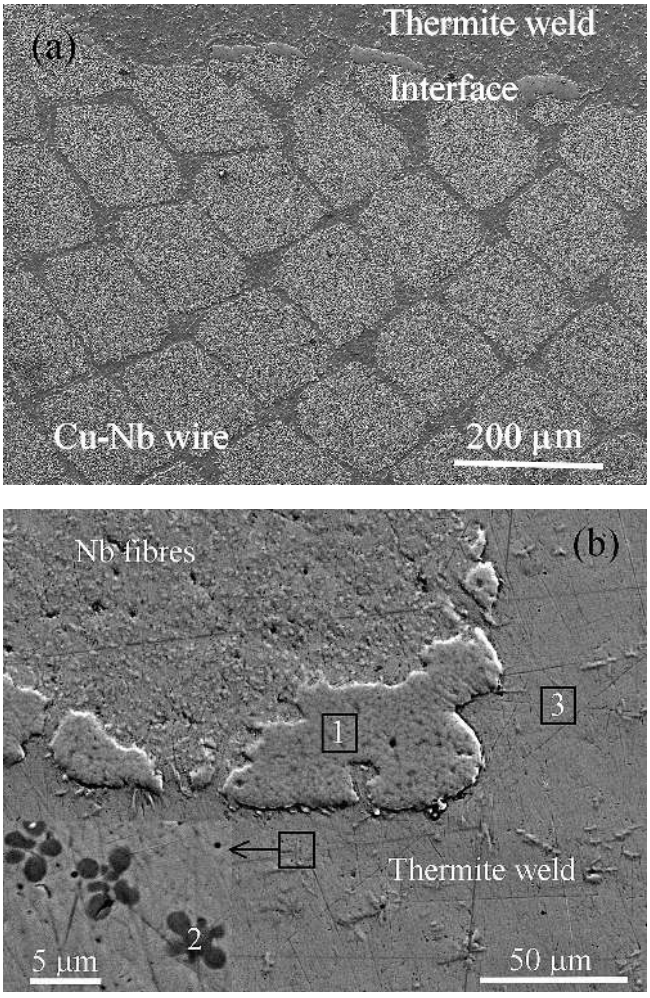

Fig. 4. Cross-section of the thermite welded joint: (a) microstucture near interface between the conductor and the weld; (b) enlarged SEM views of microstructure with the denoted EDS regions.

Table 2. The chemical compositions (by EDS) of regions 1–3 denoted in Fig. 4b (in wt.%).

Region	Chemical elements				
	Fe	Cu	Nb	Sn	Other
1	5.08	14.19	76.87	0.03	3.22
2	72.28	23.40	0.19	0.00	4.13
3	0.65	98.08	0.00	0.21	0.80

Sn content less than 5 wt.% are single-phase (α-solid solution) alloys. Since the amount of Sn in the weld did not exceed 5 wt.%, brittle secondary phases were not formed in the Cu matrix [40]. Melting of the thin Fe–Sn insert and its mixing with the liquid products of the thermite reaction explains the presence of Fe in the weld composition. The average amount of Fe is about 0.65 wt.% of the thermite weld weight (Table 2), but the solubility of Fe in the Cu matrix at room temperature is limited to 0.25 wt.% [39]. Therefore, the Fe-rich phase (denoted 2 in Fig. 4b) precipitated from the Cu-based matrix. This is a typical structure for Cu–Sn–Fe–Nb alloys, consistent with the Cu–Nb, Cu–Sn, and Cu–Fe phase transition diagrams [39]. As can be seen from the cross-section view of the thermite welding joint (Fig. 4a), the Cu–Nb conductor wire was not melted. The microcomposite wire retained its shape and microstructure. This means that joining of conductors was carried out with a very high welding process speed. Thin copper cladding, which covered the surface of the initial Cu–Nb conductor, was not observed during microscopic analysis indicating that it was melted and intermixed with the weld metal during thermite welding. The melted regions at the interface between the conductor and the weld (denoted 1 in Fig. 4b) suggest that the surface layers of the conductor were melted as well. According to EDS, this is an Nb-rich phase, which could be formed due to melting of the individual Nb fibres at the surface layer of the conductor. It is possible that the real temperature of the thermite reaction exceeded the Nb melting point (2469 °C). Besides Nb, these melted regions also contained ~14% Cu, ~5% Fe, and ~3.2% other elements. Since Cu and Nb have a negligibly low mutual solubility in the solid state, these melted regions consist mostly of two phases – Cu-rich and Nb-rich terminal solid solutions.

Thus, the joint formed from Cu–Nb wire retained its initial microstructure and shape and was surrounded by a Cu-rich thermite weld having the microstructure of a Cu-based solid solution with Fe-rich precipitates. Though the weld contained more than 98% Cu, the presence of Fe, Sn, and other elements may lead to a decrease in the electrical conductivity of the joint relative to the initial Cu–Nb conductor. On the other hand, such impurities may have a positive strengthening effect and provide better tensile strength to the weld relative to pure copper. The tensile strength of pure Cu in the annealed condition is about 220 MPa [41–43] and varies inversely with grain size. According to Krishna et al. [44], ultimate tensile strength of the copper alloys can be predicted with fairly good precision from Vickers hardness using the simple linear correlation $R_m = 3.353\ HV$, where HV is Vickers hardness number and R_m is tensile strength in MPa. The measured hardness of the thermite weld metal was in the range of 91 to 96 HV. Accordingly, the weld metal ultimate tensile strength, estimated from hardness, ranges from 305 to 322 MPa. That is 39–46% more, than it would be expected from the ingot consisting of pure copper. For the weld having ~100 mm^2 in cross-section, the maximum force ~36.6–38.6 kN can be predicted, i.e. the load-bearing capacity of the weld is ~3.26–3.44 times bigger than that of the initial Cu–Nb wire.

To estimate actual mechanical and electrical properties of the thermite joints obtained, several tests were carried out. The results are compared with results of previous studies [14, 35] below. The electrical properties of the welded joint and the conductor were compared by measuring the difference in their electrical resistances. The conductor (30 cm length) had an electrical resistance of 0.01 Ω at room temperature. As expected, a slight increase in resistance was obtained in a conductor with a thermite joint of the same length; the value measured was 0.011 Ω. However, the difference in electrical resistance was not significant (1.1 times) as it did not exceed 1.2 times, the value recommended for thermite welding [32]. The electrical behaviour of the thermite joint was found to be better than that of soldered and resistance welded joints. The value of electrical resistance of conductor with resistance welding joint was about 0.012 Ω. The electrical resistance of the samples containing joint soldered with copper (CuP6) solder was about 0.015 Ω, soldered with silver (Ag30Sn) solder – 0.014 Ω. Poor electrical properties of the soldered joints are defined mainly by low electrical conductivity of the solders applied: 7.2–15.5% IACS conductivity of solders versus 100% IACS of pure copper or 67–70% IACS of Cu–Nb wire.

Heating of the samples with the welded joint when electrical current flows was registered using a thermal imaging infrared camera. The temperature distributions at the beginning of this experiment and after 2 min of heating are presented in Fig. 5a and b, respectively. The temperature dif-

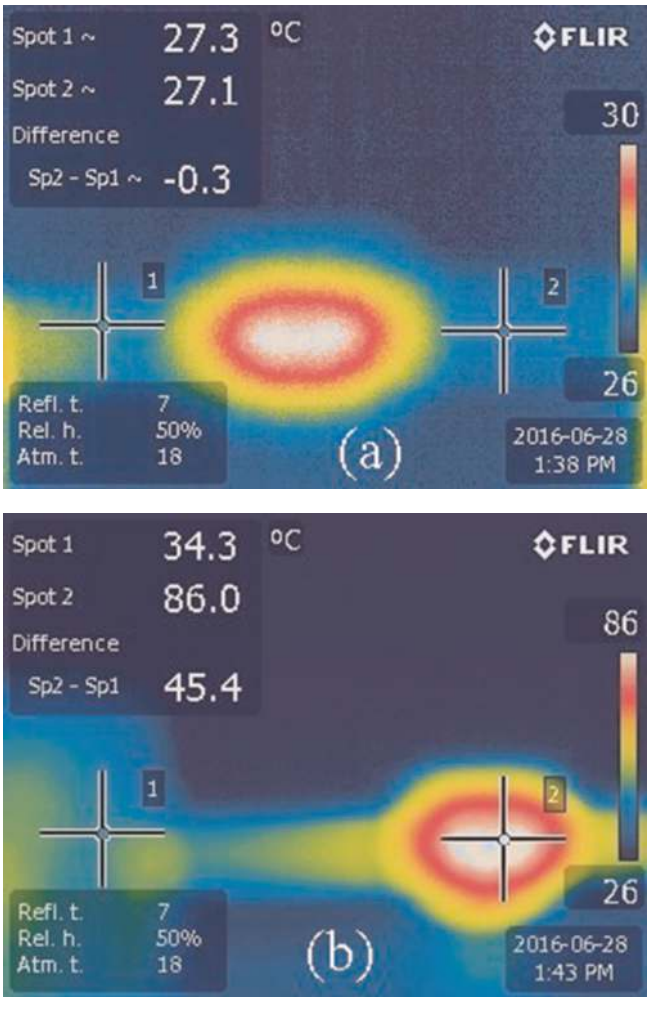

Fig. 5. View of the temperature distribution in the welded joint: (a) before heating, (b) after 2 min of heating. 1 and 2 are the points where measurements were made.

ferences in the joints and conductor when electrical current flowed did not exceed the recommended value of 95 K [32]. The most significant difference in temperatures was obtained on the joints soldered with CuP6 solder.

The stress–elongation curves obtained during the tension testing of the thermite joint are shown in Fig. 6 in comparison with curves for the initial Cu–Nb wire, soldered joint, and resistance welding joint. Obviously, the thermite connection was poorer than the initial conductor in terms of both strength and plasticity. The maximum load applied during tensile testing of the thermite joint reached 11 kN. The samples broke through the Cu–Nb conductor body near the weld (Fig. 7a), where stress concentration, caused by sudden change in the geometrical shape and local undercuts formed (Fig. 7b), takes place. The wedge-shaped fracture surface indicates that fracture was caused by shear stresses. Scanning electron micrographs, obtained under low magnification, show stair-shape surface of fracture (Fig. 7c) and presence of the dimples of different sizes (Fig. 7d), characterizing ductile overload failure in the conductor cross-section. As is known, the ductile fracture is characterised by large amounts of plastic deformation and proportionally large amounts of energy will therefore be required to induce this fracture. Therefore, when designing a structure, it is usually preferable for the material to fail in a ductile manner.

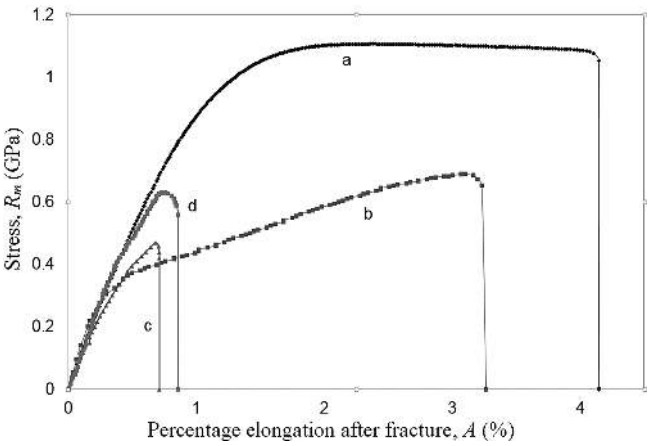

Fig. 6. Stress–elongation curve of: (a) Cu–Nb wire [35]; (b) Cu–Nb wire with thermite welding joint (break point – Cu–Nb conductor body near the weld); (c) Cu–Nb wire with resistance welding joint [14]; (d) Cu–Nb wire with soldered joint [14].

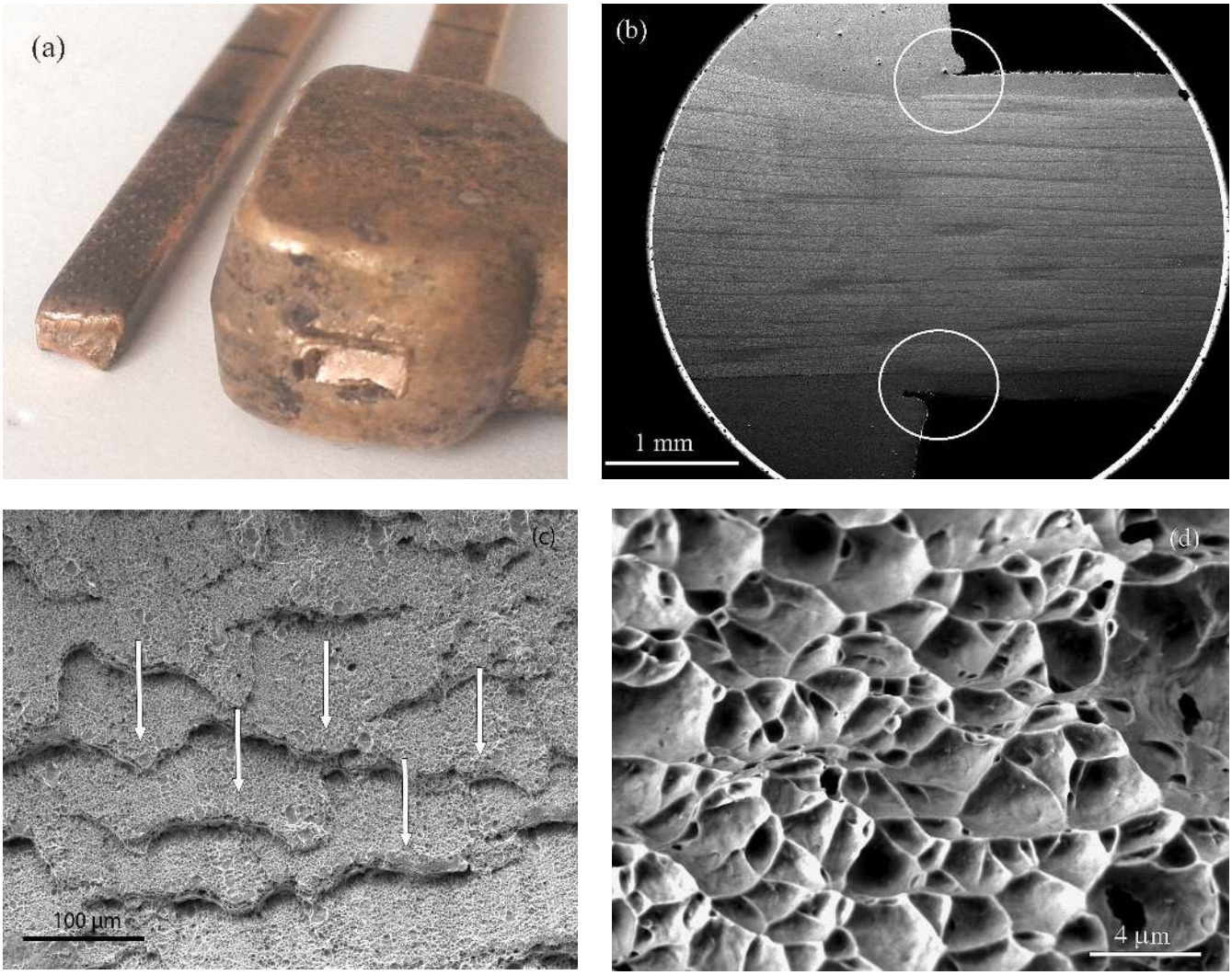

Fig. 7. Location of rupture and texture of fracture surface: (a) location of joint rupture; (b) locations of stress concentration in the cross-section of joint; (c) view of stair-shaped surface of fracture; (d) view of different sizes dimples on the fracture surface.

The maximum stress developed in the sample reached 701 MPa, equal to 62.5 % of the microcomposite wire tensile strength. The percent elongation of the welded sample after fracture was 3.2 % (or 76.2 % of the microcomposite wire percentage elongation). However, such results are much better than those obtained on the soldered and resistance welded joints. For the Cu–Nb wire joint soldered using a copper muff, the maximum load reached 6.3 kN; however, elongation after fracture (A) was only 0.85 %. During the testing of resistance welded joints a maximum load of 4.7 kN was applied and joints showed poor plasticity (0.71 %) as well. Thus, it can be stated that the thermite joint is 8 – 50 % stronger and 3.8 – 4.5 times more ductile than soldered joints and resistance welding joints. The worse mechanical properties and limited plasticity of these joints can be explained by the microstructural and geometrical peculiarities of the joints. The microstructure of the resistance weld crystallised from a melted Cu–Nb microcomposite without admixture of the welding material. The initial microstructure of the microcomposite was not retained and the microstructure of the weld consisted of Nb dendrites (18 wt.%) in Cu matrix. The shape and size of the butt resistance weld did not differ significantly from those of the wire; therefore, strengthening of the weld by increasing the cross-section was not observed in this case. The specific shape of the weld (narrow) and high microstructural gradient, typical for a resistance welding weld, also influence its mechanical properties and low resistance to bending. The soldered joint of the Cu–Nb wire was formed with the use of a copper muff; the joint was formed directly between the muff and Cu cladding of the microcomposite wire. During mechanical testing [14], the joint broke through the thin layer of solder between the muff and Cu cladding, indicating that the mechanical resistance of the whole soldered joint was limited by the properties of the solder and the length of overlap. One may assume that a particular increase in strength can be reached with other solders and by increasing the overlap length; however, it will hardly improve the plasticity of the connection. In cases where the wire with joints has to be wound into a coil or bent, the plasticity of the joint is as important as its strength. The thermite joint surpasses the soldered joint and resistance welding joint both in strength and in plasticity, and is more suitable for solenoid terminal connections with external circuits, which can withstand loads above 30 % of the conductor strength limit.

Thus, the thermite welding joint represents a Cu-based ingot (weld) with the included ends of the Cu–Nb conductor where the initial shape and microstructure of the Cu–Nb conductor are retained with minimum changes. The microstructure of the Cu-rich (>98 %) weld consists mainly of a Cu-based solid solution strengthened by Fe-rich precipitations. This structure of joint (along with its shape and size) provides insignificant increase in electrical resistance and sufficient ultimate strength and plasticity to the joint. During the tensile test, the samples broke through the Cu–Nb conductor body near the weld, indicating that stress concentration can play a particular role in joint strength. It also means that the cross-section of the weld may be reduced without loss in joint strength.

Taking into account the results of the mechanical tests and following the principle that the welded joint must be able to carry the same load as the connected elements, the cross-section of the thermite weld should be of ~ 35 mm^2 at least. To estimate experimentally the load-bearing capacity of the thermite welds with the reduced cross-section, two extra series of welded samples were prepared – with minimum (35 mm^2) and with intermediate (70 mm^2) cross-sections. During the tensile test, the behavior of "full-cross-section" joints and samples with reduced cross-sections was found to be constant: same maximum loads and elongation were reached and the samples broke in the same place of joint. Thus, the 35 mm^2 in cross-section was enough to avoid the fracture of joint through the weld. However, in order to ensure reliability of joints, a safety factor is normally introduced, which for welded joints typically is in the range of 1.4 to 1.6 [45]. Accordingly, the optimum cross-section of the thermite weld may be ~ 50 mm^2. Optimisation of the geometrical parameters of the joint in order to reduce stress concentration effects may contribute to the improvement of the properties of thermite joints. This is, undoubtedly, a task for further research.

4. Conclusions

The following conclusions can be drawn:

1. The application of appropriate thermite welding technology for Cu–Nb microcomposite conductor joining allows production of welded joints of sufficient quality. The mechanical and electrical properties of the thermite joint meet the minimum requirements for joints used in electrical engineering: the difference in electrical resistance between the conductor and welded joint does not exceed 1.2 times and the joint can withstand loads above 30 % of the conductor strength limit.
2. The applied thermite mixture (with Cu oxide and Al alloy base) ensures sufficient ignition, an appropriate reaction temperature (above 2469 °C), good slag separation and formation of a welded joint of Cu–Nb microcomposite wire.

The authors would like to thank Mr. Gunnar Mustaparda from Erico B.V., the Netherlands, for preparation of the thermite composition and fruitful discussions.

References

[1] H.E. Burke: Handbook of Magnetic Phenomena, Springer Netherlands (1986) 424. DOI:10.1007/978-94-011-7006-2
[2] F. Herlach, N. Miura: High Magnetic Fields. Magnet Technology and Experimental Techniques: Science and Technology, Vol. 1, Imperial College Press, London (2003) 336. DOI:10.1142/9789812774866_0001
[3] E. Spahn, M. Loffler, S. Balevičius: J. Korean Phys. Soc. 59 (2011) 3594 – 3598. DOI:10.3938/jkps.59.3594
[4] Z. Tesanovic: High magnetic field science and its application in the US: current status and future directions. National academies press, Washington (2013) 10. DOI:10.17226/18355
[5] G.A. Shneerson, M.I. Dolotenko, S.I. Krivosheev: Strong and Superstrong Pulsed Magnetic Fields Generation, De Gruyter Studies in Mathematical Physics, Vol. 9 (2006) 280.
[6] K. Han, J.D. Embury, J.R. Sims, L.J. Campbell, H.J. Schneider-Muntau, V.I. Pantsyrnyi, A. Shikov, A. Nikitin, A. Vorobieva: Mater. Sci. Eng. 267 (1999) 99 – 114. DOI:10.1016/S0921-5093(99)00025-8
[7] L. Brandao, K. Han, J.D. Embury, R. Walsh, V. Toplosky, S. Van Sciver: IEEE T. Appl. Supercon. 10 (2000) 1282 – 1287. DOI:10.1109/77.828470
[8] A.K. Shikov, V. Pantsyrnyi, A. Vorobeva, S. Sudev, N. Khlebova, A. Silajev, N. Belyakov: Met. Sci. Heat Treat. 44 (2002) 491 – 495. DOI:10.1023/A:1022504805662

[9] Y. Leprince-Wang, K. Han, Y. Huang, K. Yu-Zhang: Mater. Sci. Eng. 351 (2003) 214–223. DOI:10.1016/S0921-5093(02)00855-9
[10] W. Głuchowski, J.P. Stobrawa, Z.M. Rdzawski, K. Marszowski: J. Achiev. Mater. Manuf. Eng. 46 (2011) 40–49. DOI:10.1016/j.acme.2014.12.002
[11] L. Blumber, H. Hasizume, S. Ito, J. Minervini, N. Yanagi: Status of high temperature superconducting magnet development, RSFC/JA-10-45 report (2010).
[12] H. Jones, M. Van Cleemput, A.L. Hickman, D.T. Ryan, P.M. Saleh: Physica B. 246 (1998) 337–340. DOI:10.1016/S0921-4526(97)00929-0
[13] D. Ciazynski, J. Duchateau, P. Decool, P. Libeyre, B. Turck: Nucl. Fusion. 41 (2001) 223–226. DOI:10.1088/0029-5515/41/2/309
[14] N. Višniakov, J. Novickij, D. Ščekaturovienė, A. Petrauskas: Mater. Sci.-Medz. 17 (2011) 16–19. DOI:10.5755/j01.ms.17.1.242
[15] H.K. Yeo, K.H. Han: J. Alloy. Compd. 477 (2009) 278–282. DOI:10.1016/j.jallcom.2008.10.150
[16] W. Robert, Jr. Messler: Principles of Welding: Processes, Physics, Chemistry, and Metallurgy, Wiley-VCH Verlag GmbH, Weinheim (2004). DOI:10.1002/9783527617487.ch3
[17] I.G. Sharma, S.P. Chakraborty, S. Majumdar, A.C. Bidaye, A.K. Suri: J. Alloy. Compd. 336 (2002) 247–252. DOI:10.1016/S0925-8388(01)01860-6
[18] H. Wang, G. Jian, C. Garth, R.M. Zachariah: Combust. Flame. 161 (2014) 2203–2208. DOI:10.1016/j.combustflame.2014.02.003
[19] D.G. Piercey, T.M. Klapotke. Nanoscale Aluminum – Metal Oxide (Thermite) Reactions for Application in Energetic Materials. Cent. Eur. J. Energ. Mat. 7 (2010) 115–129.
[20] V.E. Sanders, B.W. Asay, T.J. Foley, B.C. Tappan, A.N. Pacheco, S.F. Son: J. Propul. Power. 23 (2007) 707–714. DOI:10.2514/1.26089
[21] L. Takacs: Prog. Mater. Sci. 47 (2002) 335–414. DOI:10.1016/S0079-6425(01)00002-0
[22] Tubefuse applications B.V. Exotermic mixture. US patent: us 20120061454 (2012).
[23] Tubefuse applications B.V. Exotermic mixture. WO patent: wo 2010046666 (2010).
[24] Erico Products, Inc. Exothermic reaction mixture and method of cast welding a copper base alloy utilizing same. US patent: us 2870499 (1959).
[25] Erico Products, Inc. Exothermic reaction mixture for producing a molten copper alloy. US patent: us 2801914 (1957).
[26] A.N. Kukin, A.A. Talikov. Exotermic mixture. USSR Certificate of Authorship: 77895 (1949) (in Russian).
[27] Ufa State Aviation Technical University. Composition for thermite welding. RU patent: ru 2371289 (2009).
[28] B.V. Ioffe. Thermit welding composition. RU patent: ru 2151037 (2000) (in Russian).
[29] A.V. Tsypin. Thermite welding compound. RU patent: ru 2357846 (2009).
[30] OOO Gazprom transgaz Samara. Composition for aluminothermic welding. RU patent: ru 2385208 (2010).
[31] D.M. Stefanescu: ASM Metal Handbook, Vol. 15: Casting. ASM International, Ohio (2008) 1256.
[32] M.V. Chomiakov, I.A. Jacobson: Thermite welding of multiwire conductors of power lines and substations. Gosenergoizdat, Moscow (1963) 80 (in Russian).
[33] J.R. Davis: Copper and copper alloys. ASM international, Ohio (2001) 869.
[34] J.P. Frick, N.E. Woldman: Woldman's engineering alloys. 9th edition. ASM international, Ohio (2000) 861.
[35] N. Višniakov, J. Novickij, D. Ščekaturovienė, M. Šukšta: Sol. St. Phen. 113 (2006) 541–544. DOI:10.4028/www.scientific.net/SSP.113.541
[36] H. Mao, M. Hillert, M. Selleby, B. Sundman: J. Am. Ceram. Soc. 89 (2006) 298–308. DOI:10.1111/j.1551-2916.2005.00698.x
[37] GOST 17441-84. Electrical contact connections. Acceptance rules and methods of tests. Moscow, 1984 (in Russian).
[38] GOST 10434-82. Electrical contact connections. Classification. General technical requirements. Moscow, 1982 (in Russian).
[39] P. Franke, D. Neuschütz: Thermodynamic Properties of Inorganic Materials: Binary Systems. Part 3: Elements and Binary Systems from Cs–K to Mg–Zr, Springer-Verlag, Berlin (2005) 309. DOI:10.1007/b76784
[40] M.D. Maltsev: Metallography of industrial non-ferrous metals and alloys, Metallurgy, Moscow (1970) 178 (in Russian).
[41] O.E. Isincev: Copper and copper alloys. Native and foreign marks. Reference book, Mashinostrojenije, Moscow (2004) 336 (in Russian).
[42] W. Martienssen, H. Warlimont. Springer Handbook of Condensed Matter and Materials Data. Springer Science & Business Media (2006) 1121.
[43] V.J. Kershenbaum. International Translator of Modern steels and alloys. Volume 3. International academy of Engineering. Intac Ltd (1993) 635 (ijn Russian).
[44] S.C. Krishna, N.K. Gangwar, A.K. Jha, B. Pant: J. Mater. (2013) 1–6. DOI:10.1155/2013/352578
[45] A. Nedoseka: Fundamentals of Evaluation and Diagnostics of Welded Structures.Woodhead Publishing (2012) 639. DOI:10.1533/9780857097576

(Received December 8, 2016; accepted June 16, 2017)

Correspondence address

Dr. Nikolaj Višniakov
Faculty of Mechanics
Vilnius Gediminas Technical University
Basanavičiaus str. 28
03224 Vilnius
Lithuania
Tel.: +370 5 2745053
Fax: +370 5 2744740
E-mail: nikolaj.visniakov@vgtu.lt

Bibliography
DOI 10.3139/146.111554
Int. J. Mater. Res. (formerly Z. Metallkd.)
108 (2017) E; page 1–8

ISSN 1862-5282